Pergamon

Available online at www.sciencedirect.com

SCIENCE DIRECT®

Acta Materialia 51 (2003) 5881–5905

Acta MATERIALIA

www.actamat-journals.com

The biomechanics toolbox: experimental approaches for living cells and biomolecules[☆]

K.J. Van Vliet [a,b,*], G. Bao [c], S. Suresh [a]

[a] *Department of Materials Science and Engineering, Massachusetts Institute of Technology, Cambridge, MA 02139, USA*
[b] *Department of Surgical Research, Children's Hospital and Harvard Medical School, Boston, MA 02115, USA*
[c] *Department of Biomedical Engineering, Georgia Institute of Technology and Emory University, Atlanta, GA 30332, USA*

Accepted 31 August 2003

Abstract

The mechanical behavior of biological materials has been studied extensively at the tissue, organ and systems levels. Emerging experimental tools, however, enable quantitative studies of deformation of individual cells and biomolecules. These approaches also facilitate the exploration of biological processes mediated by mechanical signals, with force and displacement resolutions of 0.1 pN and 0.1 nm, respectively. As a result of these capabilities, it is now possible to establish the structure-function relationships among the various components of a living cell. In order to fully realize this potential, it is necessary to critically assess the capabilities of current experimental methods in elucidating whether and how the mechanics of living cells and biomolecules, under physiological and pathological conditions, plays a major role in health and disease. Here, we review the operating principles, advantages and limitations, and illustrative examples of micro- and nano-scale mechanical testing techniques developed across many research communities to manipulate cell populations, single cells, and single biomolecules. Further, we discuss key opportunities for improved analysis of such experiments, as well as future directions and applications.

© 2003 Acta Materialia Inc. Published by Elsevier Ltd. All rights reserved.

Keywords: Biomechanics; Macromolecular materials; Elastic behavior; Stress-rupture

1. Introduction

The structure and function of many living cells depend directly on their global and local mechanical environment. The importance of this mechanical stimulus can be appreciated at the tissue level through well-known examples such as muscle atrophy and bone resorption in the absence of skeletal loading, and has been implicated at the cellular level in terms of processes including adhesion, motility and differentiation. Fundamental understanding of these basic cellular processes, and of the pathological responses of the cell, will be facilitated greatly by developments in the fields of cell and molecular biomechanics. Despite the sophistication of experimental and computational approaches in cell and molecular biology, the mechanisms by which cells sense and respond to

---

[*] Corresponding author.
E-mail address: krystyn@mit.edu (K.J. Van Vliet).

[☆] The Golden Jubilee Issue—Selected topics in Materials Science and Engineering: Past, Present and Future, edited by S. Suresh.

1359-6454/$30.00 © 2003 Acta Materialia Inc. Published by Elsevier Ltd. All rights reserved.
doi:10.1016/j.actamat.2003.09.001

mechanical stimuli are poorly understood. To a large extent, the intricate coupling between the biochemical and mechanical processes of the cell impedes research efforts. In particular, application of external mechanical stimuli can induce biochemical reactions, including the synthesis of new biomolecules and the enhanced interaction among biomolecules that can generate mechanical forces. Likewise, changes in chemical stimuli, including pH, temperature, and biomolecular activity, can alter the structure and mechanical integrity of the cell, even in the absence of mechanical stimuli.

In contrast with most material systems, the mechanical behavior of a living cell cannot be characterized simply in terms of fixed “properties”, as the cell structure is a dynamic system that adapts to its local mechanochemical environment. Mechanistic understanding of the relationships among extracellular environment and intracellular structure and function, however, requires meaningful quantification of these closely coupled fields. To that end, researchers from such diverse disciplines as molecular biology, biophysics, materials science, chemical, mechanical and biomedical engineering have developed an impressive array of experimental tools that can measure and impose forces as small as a few fN (10^{-15} N) and displacements as small as a few Angstroms (10^{-10} m). Thus, it is now possible to probe the interaction forces between individual molecules that comprise the cell and its local environment, as well as the mechanical response of the entire cell (See Fig. 1 for schematics of prokaryotic and eukaryotic cells, as well as key molecules, that have been analyzed experimentally with these tools).

Due to the rich history and unique perspectives of the fields that contribute to advances in the experimental mechanics of living cells and biomolecules, the questions of interest, approaches, tools and even vocabulary particular to these communities can impede communication and progress in this inherently interdisciplinary venture. To this end, we review in detail experimental tools and associated analytical/computational models with the aim to identify opportunities and challenges for interdisciplinary collaboration and achievements in this important field of experimental micro- and nanomechanics of biological materials.

There exist a variety of techniques to manipulate the mechanical environment of cell populations, individual living cells, and individual biomolecules. These approaches differ in three important respects: operating principles, force and displacement maxima and resolutions, and extent of deformation (i.e., global vs. local). Table 1 summarizes the abbreviations, relevance to biological structures, and applications for each of the experimental tools discussed below. Fig. 2 indicates the range of force and displacement covered by these approaches, as compared to the range relevant to representative biological structures/processes.

2. Cell population techniques

This section begins with a consideration of studies that focus on the mechanical response or mechanical manipulation of entire cell populations. Here, the purpose is often to understand the role that mechanics plays in regulating the structure and function of tissues that comprise organs.

2.1. Substrate deformation

Direct manipulation of the substrate to which cells adhere (substrate deformation, or SD) provides a means of mechanical stimulation. Here, strains are imposed and measured via standard strain gages or other low-resolution displacement sensors, and global forces are calculated directly from strain gage output and/or experimentally determined substrate stiffness. Maximum applied force and displacement are in the Newton range (with resolution of 1 mN) and mm range (with resolution of 1 μm), respectively. This in vitro approach has been adapted by researchers in an attempt to impose static and cyclic deformation representative of in vivo conditions, and thus the methods and objectives of such substrate manipulation studies are peculiar to the cell type of interest [27-30,105]. Since osteoblasts (bone cells) and chondrocytes (cartilage cells) are known to react to mechanical stimuli, earlier work was concentrated in the orthopedics and traditional (continuum) biomechanics fields (e.g., Ref. [31]). More recently, this method has been applied to

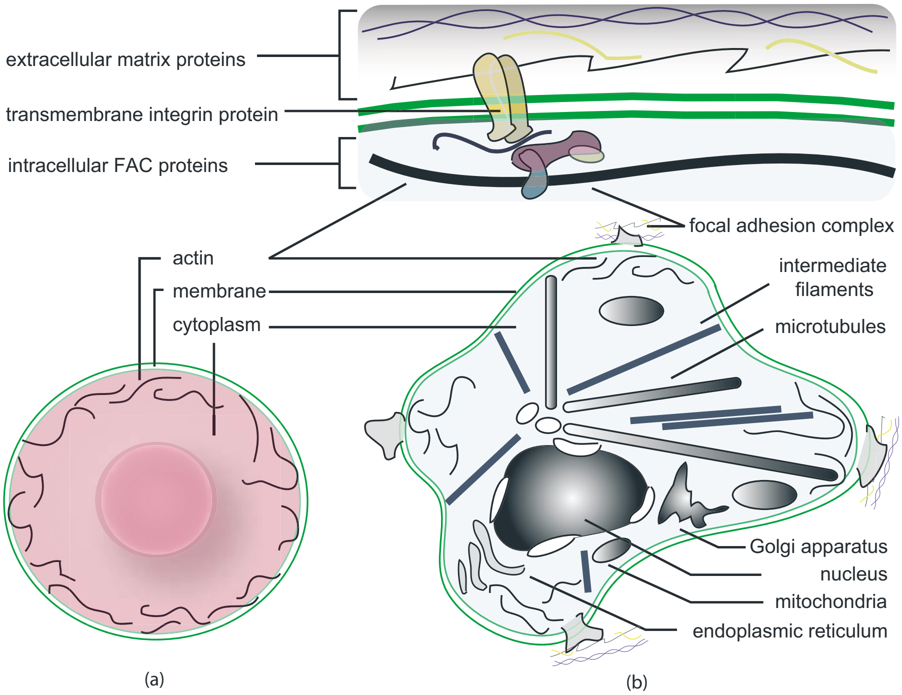
extracellular matrix proteins
transmembrane integrin protein
intracellular FAC proteins
focal adhesion complex
actin
membrane
cytoplasm
intermediate filaments
microtubules
Golgi apparatus
nucleus
mitochondria
endoplasmic reticulum
(a)
(b)

Fig. 1. (a) Prokaryotic cell such as an erythrocyte; (b) Eukaryotic cell such as a fibroblast, with molecular detail of focal adhesion complexes (FACs) whereby such adherent cells interact with the extracellular matrix (ECM).

Table 1
Applications of experimental approaches in cell/molecular mechanics and relevant nomenclature

Application	Technique	Abbreviation	Example
Cell population	Substrate deformation	SD	Effects of global stress on cell morphology [1]
Cell population & single cell	Substrate composition	SC	Effects of substrate stiffness on cell motility [2]
	Embedded particle tracking	EPT	Measuring cell migration forces [3]
	Microfabricated post array detector	mPAD	Measuring inter/intracellular traction [4]
	Magnetic twisting cytometry	MTC	Characterizing frequency dependence of cellulr components [5-7]
Single cell	Cytodetacher	CD	Measure cell-substrate adhesion forces [8]
	Micropipette aspiration	MA	Viscoelastic properties of erythrocyte cortex [9,10]
	Optical stretcher	OS	Noncontact, large deformation of cells [11]
Single cell & single molecule	Atomic force microscopy	AFM	Cell / cytoskeletal protein stiffness [12-17]
	High resolution force spectroscopy	HRFS	Measure ligand-receptor unbinding forces [18,19]
	Microneedle	MN	Qualitative cell stiffness during migration [20,21]
	Optical tweezers	OT	Effect of disease state on erythrocyte elasticity [22]
	Magnetic tweezers	MT	Viscoelastic deformation of cells and membranes [23-26]
	Biomembrane force probe	BFP	Ligand-receptor unbinding [9]

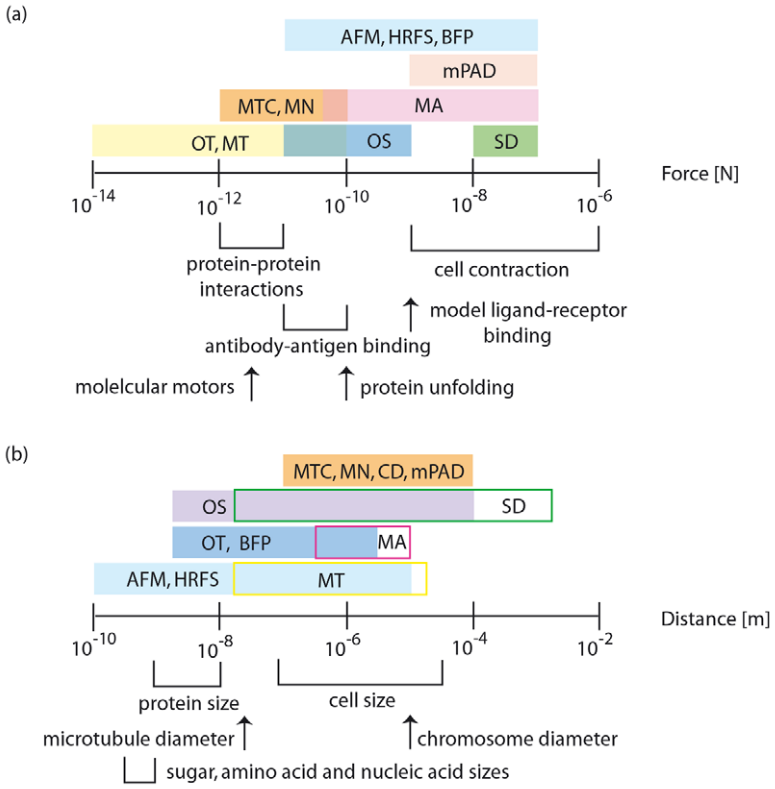

Fig. 2. (a) Force range of experimental techniques and biological events; (b) Displacement range of experimental techniques and dimensions of biological structures.

studies of endothelial cells [32] and melanocytes [33] under cyclic strain, as well as stretch-induced injury of neurons [34].

One example of this approach is shown in Fig. 3. The uniaxial stretching device shown in Fig. 3(a) consists of a voice coil actuator that imposes displacement, a linear encoder that measures displacement, a proportional-integral-derivative (PID) controller/amplifer, a power supply and a computer interface [34]. The actuator, which is capable of imposing displacements of up to 2 cm at high rates, is mounted on a linear bearing slide and is controlled by the PID feedback loop with the linear encoder. This displacement-controlled SD apparatus can attain strains >70% and strain rates of up to 90 s^{-1}. As illustrated in Fig. 3(b), this device imposes global strain via uniaxial displacement of an elastic substrate on which cells are maintained in two-dimensional (2D) culture. Here, cells are seeded on a thin (130 μm) silicone membrane that is mounted between a glass cover slip and a thick (1.5 mm) silicone layer that includes a well. This well contains pH-buffered, nutrient-enriched media so that experiments can be conducted in vitro (i.e., cultured at physiological temperature and %CO_2), and defines the gage length of the substrate. In this manner, the substrate can be deformed over a loading profile specified by the user. Thus, cells can be maintained in vitro under various uniaxial loads and the effect of this deformation on the morphology, genetic regulation (via standard molecular biology techniques such as polymerase chain reaction or PCR), metabolic activity (via analysis of molecules excreted by the cells into the media), injury and even cell phenotype (via staining with cell-specific surface markers) can be assessed.

2.2. Substrate composition

An alternative means of providing mechanical stimuli to a cell population through substrate

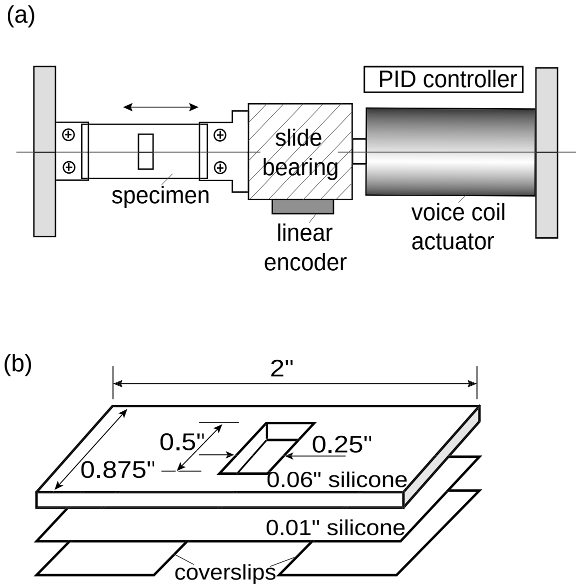

Fig. 3. Substrate deformation (SD) for cell population studies. (a) An example apparatus consisting of a voice coil displacement actuator and a linear encoder displacement sensor in proportional-integral-derivative (PID) feedback. The substrate can be deformed uniaxially according to a specified displacement profile. (b) Schematic of substrate fluid chamber that can maintain cells in vitro by culturing them on a compliant silicone membrane fixed between a thicker silicone membrane containing a well and rigid glass cover slips.

manipulation is by controlling the chemical composition of the substrate material and thereby affecting the mechanical properties of the substrate. This can be done by varying the concentration of one component or extent of crosslinking in a polymeric gel [2], or by varying the entire composition of the substrate (e.g., collagen gel vs. synthetic polymeric gel). In both cases, it is important to maintain the same chemical environment (species, hydration, adhesivity, etc.) of the cell population, including the concentration and activity of molecules at the substrate surface that will interact directly with the cells [35]. This requirement can be met by coating each of the various substrates with the same ECM proteins, for example. In addition, the thickness of a substrate of fixed composition could be varied systematically to affect the maximum compliance of the substrate to which the cells adhere. As this technique is applied mainly to study cell motility, the effective elastic modulus of the substrate is determined experimentally via uniaxial tension, but force and deflection imposed by the cell(s) are not quantified.

In an interesting set of SC experiments, Lo et al. [36] have created a polyacrylamide gel for which the polyacrylamide concentration and thus the elastic compliance change at a well-defined interface, and seeded fish fibroblasts onto one side of this ECM-coated substrate. They observed visually the adhesion and motility of these cells in vitro (see Fig. 4). Through this cell population experiment, it was shown that these cells would actively migrate from a substrate of relatively low compliance toward a substrate of relatively high compliance, but would not migrate readily in the opposite manner. In fact, as evident from the real time imaging of this cell migration study [37], cells

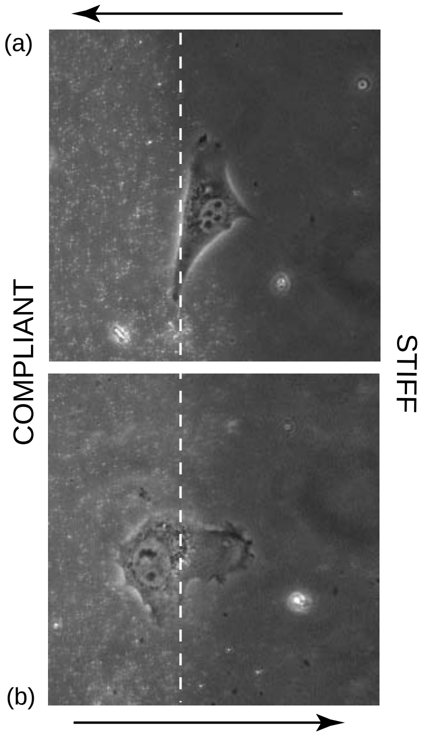

Fig. 4. Cell population study of migration (arrows) via variation of substrate composition (SC). Dashed line indicates division between relatively stiff and compliant polyacrylamide substrates. (a) Fibroblast migrating from stiffer to more compliant region; (b) Fibroblast migrating from more compliant to stiffer region. Note the effect of substrate compliance on cell morphology. Images courtesy of C.-M. Lo and Y.-L. Wang.

approaching the interface immediately change direction and migrate opposite the region of lower compliance. Furthermore, cells moved toward a region of localized tension in the substrate (pulling on a blunted micropipette submerged in the gel) and away from a region of localized compression (pushing on that micropipette). Although the molecular mechanism by which the cells sense the difference in mechanical stiffness of the substrate is not fully understood, related research [2] has shown that myosin motors play a role in enabling the cell to sense the local mechanical stiffness through focal adhesion complexes (FACs) and that increased substrate stiffness correlates with increased phosphorylation of tyrosine. This molecular modification appears critical to the formation of stable FACs as shown in Fig. 1. Thus, such cell population studies are important in the sense that they can show both the individual and collective behavior of cells through cell/substrate interactions.

The methods outlined above consider the cells in a 2D culture system, whereas cells in vivo are typically contained within a three-dimensional (3D) ECM. In theory, each of these methods could be extended to 3D. In practice, however, this critical aspect of the cell environment is limited by the difficulty associated with imaging and manipulating cells in 3D. Efforts to overcome this limitation will extend the utility of such cell population studies.

3. Single cell and single molecule techniques

One criticism of cell population studies such as those described above is that, despite the ability of such studies to show that applied mechanical stress alters cell structure and function, the heterogeneity among cell responses is largely ignored. Furthermore, the response of a single cell to mechanical signals (i.e., mechanisms of cellular deformation and mechanotransduction) cannot be decoupled easily from the response of the entire population. In this section, we discuss advances in the manipulation of individual living cells, whereby the manipulation of the environment of a single cell can help elucidate how a cell receives and processes extracellular mechanical signals. Further, we illustrate how some of the same experimental methods can be applied to the studies of single-molecule biomechanics.

3.1. Embedded particle tracking

By embedding micro-scale beads within a polymeric substrate, traction forces exerted by adherent cells can be measured at many points of cell-surface contact. Here, the beads serve as fiduciary markers within a flexible membrane [38]. The displacement of the beads x is measured optically, and the corresponding force F is calculated via the experimentally determined elastic stiffness k of the membrane:

$$F = -kx. \tag{1}$$

As this force is derived from the traction between the adherent cell and its substrate, this method is also commonly referred to as traction force microscopy [39]. The displacement resolution of this technique is limited by the available optics; the force resolution is limited by available optics as well as the accuracy of k. The value of k can be estimated by simple mechanical tension experiments such as the optically measured deflection of the membrane via a known mass [2], or via techniques such as microneedle (MN, Section 3.7) or nanoindentation, and typically neglect elastic nonlinearity and time-dependent responses of the membrane. Further, the deconvolution of bead displacement to force maps has been a major analytical challenge but, as shown in Fig. 5, can now be resolved at the sub-micron scale to identify molecular sites of cell-substrate adhesion that comprise FACs. Note that this technique, like the majority of substrate interaction techniques, is confined to adherent cells in 2D culture. In principle, optical deconvolution of 3D bead displacement would allow through-thickness determination of traction forces in 3D experiments.

3.2. Magnetic twisting cytometry

Magnetic twisting cytometry (MTC) also relies on the use of beads to measure pointwise displacement, but this method differs from EPT in two

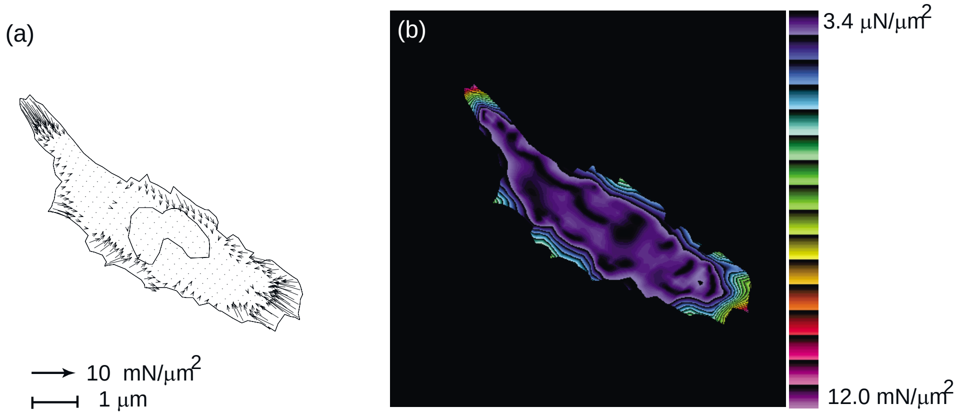

Fig. 5. Embedded particle tracking (EPT) for single cell and cell population studies. (a) Arrows indicate magnitude and direction of traction calculated from particle displacement for a fish fibroblast on polyacrylamide substrate. (b) Conversion of vector data in (a) to color-encoded map, where hot colors indicated large traction and cool colors indicated small traction forces over the entire cell. Images courtesy of K. A. Beningo and Y.-L. Wang.

important respects. Firstly, in MTC the cells partially phagocytose (engulf) ferromagnetic beads ranging in diameter from 250 nm to 5 μm; the substrate does not contain embedded beads. Secondly, in MTC the beads impose cell displacement, whereas in EPT the cells impose bead displacement. The method of MTC was developed by Crick et al. [24] to study the properties of the cytoplasm and has been used more recently to study the mechanics of the cell membrane and the cytoskeleton [40], particularly under cyclic loading conditions [5,6,41]. Here, large numbers of magnetic beads (~ 5 μm in diameter) are coated with ligands chosen specifically to bind to cell surface receptors such as integrin that are known to interact with the cytoskeleton. Shortly after these ligand-coated beads are introduced to the cell culture, a weak external magnetic field H_1 is applied to align the remnant magnetic fields B_1 of the individual beads. Upon bead attachment to the cell surface, the cell is subjected to an external magnetic field H_2 normal to the substrate. This field causes the beads to rotate, resulting in a highly nonlinear and variable stress field according to the total number, distribution, and B_1 of the attached beads. This rotation is measured via magnetometry as the magnitude of the remnant magnetic field B_2, and the corresponding torque F_T is calculated:

$$F_T = cH(t)\cos\phi(t). \tag{2}$$

where c is an experimentally determined bead calibration constant measured in a medium of known viscosity such as glycerol (see Section 3.4), ϕ is the angle between the remnant fields B_2 and B_1, and $H(t)$ represents the amplitude H_a and frequency ω of the applied field $H_a\sin(\omega t)$. Note that displacement is not measured directly, but is calculated from the magnetic signal $B(t)$ (Fig. 6).

During these experiments, the cell sample can be rotated at a low frequency (~10 Hz) to reduce the magnetic signal to noise ratio [6], requiring demodulation of the output signal according to a time or frequency domain algorithm. This involved and restrictive identification of the magnetic signal limits the frequencies of cell deformation that can be studied and also complicates the interpretation of the data. However, the time dependence inherent to this technique makes MTC well suited to the viscoelastic characterization of single cells and also cell populations, including estimation of elastic storage and loss moduli, over frequencies ranging from 0.2 to 400 Hz [6]. Furthermore, as the beads can be tailored to attach to specific cell surface receptors, various hypotheses about how the cell communicates with the ECM can be tested experimentally [33].

One application of MTC is the estimation of the storage modulus G' and loss modulus G'' of (contractile) human airway cell populations for

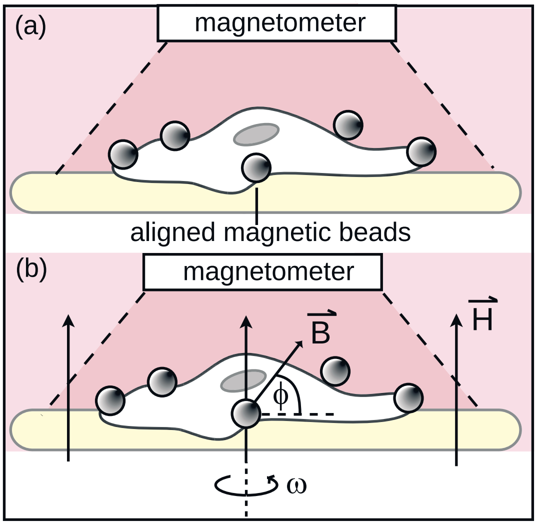

Fig. 6. Magnetic twisting cytometry (MTC) for single cell studies. (a) Micro- to nanoscale ferromagnetic beads attach aspecifically or specifically to the cell membrane and are briefly magnetized to align magnetic dipoles. (b) A magnetic field H is applied to induce bead rotation ϕ, and the corresponding remnant field of this rotation B is measured via a magnetometer. To increase the magnetic signal/noise ratio, the sample is rotated about the H direction at an angular velocity ω.(After Ref. [6]).

which magnetic beads are bound to transmembrane integrin receptors, components of the FACs as shown in Fig. 1 [7]. Maksym et al. found that these moduli were weakly dependent on frequency, and tracked changes in these parameters as a function of chemical environment to show that cytoskeletal disruption reduces the storage and dissipation of energy proportionally in this cultured cell population.

3.3. Micropatterned substrates

Several cell manipulation technologies have been enabled by the development of thin film lithographic techniques. Here, micropatterned substrates are fabricated to allow pointwise control of cell adhesion and traction measurement through displacement of the pattern features [42-44]. One interesting example of this approach is the microfabricated post array detector (mPAD) . Tan et al. [4] have produced an array of independently deforming posts onto which cells can adhere by using standard photolithography to create a silicon replica, then casting an elastomer (PDMS) within that replica to form a pattern of flexible micron-scale cantilevers (oriented vertically), and finally microcontact printing [45] the cantilever ends with ECM protein to facilitate cell adhesion. With this patterned substrate, these authors have shown that the cell forms FACs at the points of contact with these cantilevers and deflects them toward the cell center. The stiffness of the cantilevers can be controlled by varying either the stiffness of the elastomer or the geometry of the cantilever. The deflection x imposed by the cell, measured via image analysis, has been related to the force F via the standard linear elastic beam theory:

$$F = 3EIx/L^3 \tag{3}$$

where E is the (time-independent) elastic modulus, I is moment of inertia, and L is and the cantilever beam length. Here, the strain imposed on a particular cell cannot be modulated in a given experiment; it is set by the compliance of the cantilever array. In addition, the deformation is quantified only in the plane of the cell/post interface; changes normal to this plane (cell thickness) cannot be assessed. However, this method is advantageous in that mPAD resolves the deformation imposed by the cell at sub-cellular (9 μm) scales, and can thus map the corresponding, spatially varying traction forces with a resolution of 12 nN, as shown in Fig. 7. It has been shown [4] that the traction forces increased as the FAC size increased, at least as this FAC size was quantified through fluorescence of a particular ECM protein. Although they did not consider the deformation in terms of stress and strain, Tan et al. reported that when they constrained the area over which cells could adhere (by defining the number of ECM-coated posts), “small” cells exhibited less traction force than “large” cells, indicating that the number of FACs that the cell can form contributes directly to the level of stress that the cell can impose on its substrate. Note that Eq. (3) is a time-independent, linear relation, and its application in the mPAD analysis neglects the hyperelastic and viscoelastic deformation/creep of the elastomer. This consideration may be especially important when examining

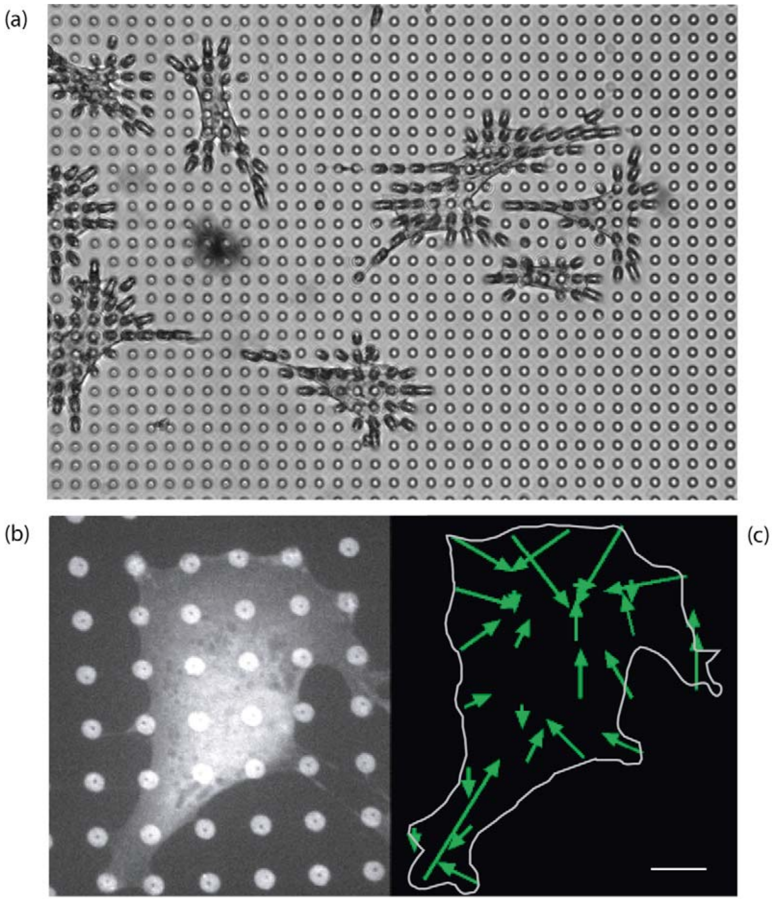

Fig. 7. The Microfabricated Post Array Detector (mPAD), an example of micropatterned substrates for cell population and single cell studies. (a) NIH3T3 fibroblasts on post array of 9 μm spacing; (b) Phase contrast image of single fibroblast; (c) Vector map of force calculated from post deflection. Scalebar = 50 nN. Images courtesy of J. Tan and C. Chen.

the response of the cell over time spans of chemical exposure.

3.4. Micropipette aspiration

The micropipette aspiration technique (MA) has been used widely to study time-dependent deformation of living, individual cells subjected to extracellular pressure. Here, the cell is drawn into a glass tube, the inner diameter of which is a chosen fraction of the nominal diameter of the cell, via stepwise application of aspiration pressure $\triangle p$ (i.e., suction). Applied aspiration pressure ranges from 0.1-1000 Pa, with resolution of 0.1 Pa [10,46]. This pressure is maintained over a specified duration, and the attendant extension of the cell into the pipette is monitored via optical microscopy. Displacement of the cell membrane is tracked by light microscopy with a claimed resolution of ± 25 nm [46]. The micropipettes and glass walls that define the fluid cell of the experiment are coated with 1% agar to inhibit cell adhesion. Thus, MA enables real-time correlation of pressure and whole-cell deformation. Force F is related to applied aspiration pressure and membrane deflection as:

$$F = \pi R_p^2 \Delta p(1 - [x'_p / x'_a] \qquad (4)$$

where R_p is the micropipette radius, and x'_p and x'_a are the velocities of the cell in the presence and absence of applied aspiration pressure Δp, respectively [47]. Through application of a chosen viscoelastic model for the cell membrane, MA-induced deformation is used to calculate elastic modulus E, apparent viscosity μ for the cell membrane and time constants of deformation and/or relaxation τ.

Such experiments [46,48,49] have been developed to measure the viscoelastic behavior of the cells that flow and deform in narrow channels during physiological function, including erythrocytes (red blood cells), and granulocytes and neutrophils (two types of white blood cells). In addition, MA has been applied to discern the viscoelastic contribution of the cortex, or outermost region of the cytoplasm that is rich in the cytoskeletal protein actin [9,10]. This experimental approach has also been applied to cell types that are present in load-bearing tissues such as cartilage. Here, the motivation is that fluid flow and stress distributions in cartilage depend on the unknown mechanical properties of chondrocytes. As shown in Fig. 8, Jones et al. [50] employed micropipette aspiration to compare the calculated elastic modulus E and magnitude of pressure-induced volume change in chondrocytes derived from normal and osteoarthritic articular cartilage. No statistically significant difference was observed between cells derived from normal and abnormal tissue in the value of E calculated from their data with a continuum-based elastic half-space model (E = 0.7 kPa). However, a marked difference was observed in the volume change sustained upon complete aspiration of the chondrocyte within a micropipette: under strains ranging from 10-45%, mean volume decreased by 11 and 20% in chondrocytes derived from normal and osteoarthritic cartilage, respectively.

From these examples, it is clear that MA is a useful approach for cell types that undergo large, general deformation that contributes critically to cell and/or tissue function. Although the applied stress state is relatively complex and based largely on fluid mechanics, continuum approximations have commonly been used to extract the mechanical and functional characteristics of the cell deformed by aspiration. Analytical models of viscoelasticity in erythrocytes [51,52] and chondrocytes [53], though useful for constructing hypotheses that can be tested via MA, are restricted by the many assumptions required for mathematical tractability. Computational models of MA cell deformation include finite element modeling (FEM) [54,55] and boundary integral modeling

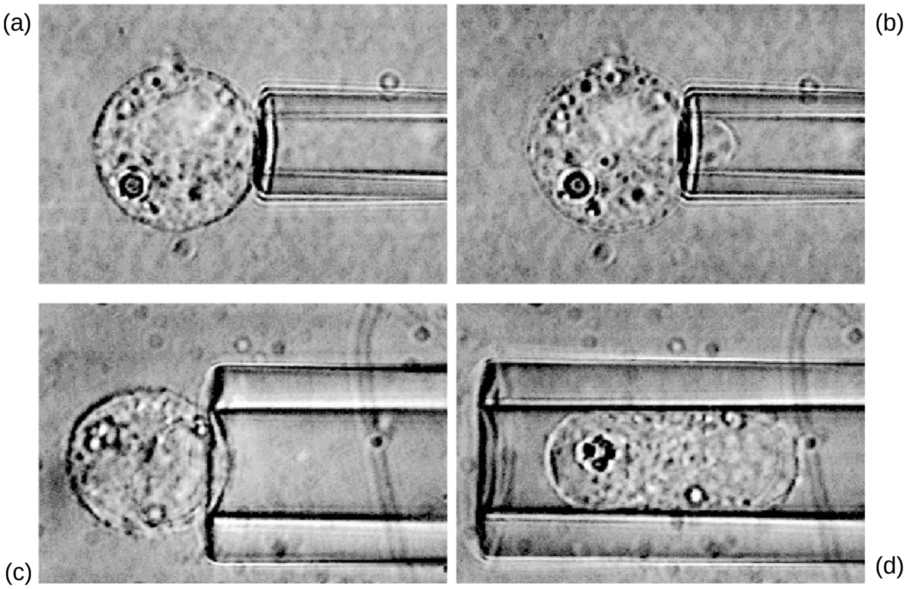

Fig. 8. Micropipette aspiration (MA) for single cell studies in chondrocytes. (a, b) Cell elasticity experiment; (c, d) Whole cell compressibility experiment. Images courtesy of F. Guilak, used with permission from Elsevier, Ref. [50].

(BIM) [56,57]. Increasingly, these models incorporate biphasic, or layered, structural assumptions that delineate the contributions of the cortex and of the cytoplasm. As the predictions of these models depend on the choice of constitutive model, including the value of mechanical properties and time constants, the chief use of these simulations is to fit experimental data to a given constitutive model and thereby obtain estimates for elastic and viscous properties. Clearly, the choice of constitutive model dramatically affects the value of fitted parameters, i.e., the calculated viscoelastic characteristics. While the vast majority of constitutive models used to interpret MA aspiration experiments have been based on continuum formulations, molecular dynamics analysis of the cell membrane spectrin network using Monte Carlo simulations have also been developed in recent years [58-60].

3.5. Optical traps

Several experimental approaches developed to investigate single cell mechanics are based on the controlled displacement of dielectric objects that are either attached to the cell membrane or placed inside the cell [61,62]. Such devices, termed single-beam gradient optical traps (OT), optical tweezers, laser tweezers or optical clamps, rely on the conservation of photon momentum. That is, when transmitted through a dielectric object of high refractive index n_o and of radius $R \gg$ laser wavelength λ, the photons from a focused laser beam are subject to a change in momentum as a consequence of refraction when the beam enters and exits the object. This momentum change, in turn, exerts a restoring force F_g on the object (recoil) in the direction of greater photon flux (i.e., toward the center of the photon intensity gradient that is in fact the focal point of the laser beam). This optical trap is stabilized with respect to repulsive forces when the gradient along the axis of the laser dominates over all other gradients, which is why lenses of large numerical aperture (*NA*) are required. As a result, the dielectric object moves toward the laser focal point under a force F_g, and can thus be used to impose force through translation of the focal point or to measure externally applied force through the resulting motion of the trapped object:

$$F_g = -kx \qquad (5)$$

where k is the optical trap stiffness and x is the bead displacement due to momentum conservation, measured via image analysis, optical interference patterns, or position-sensitive photodiodes that track refracted laser light [63]. Note that the scattering force utilized in OT is the difference between the attractive force due to refraction and the repulsive force due to reflection. The value of k can be tailored by varying the trap design (laser power P, NA, and R) and is on the order of 50 pN/µm. For an excellent review of the physics of optical traps, we refer the reader to Refs. [64,65].

This phenomenon is a general effect of light on all objects, but the resulting forces are typically negligible. For example, the repulsive radiation pressure exerted by a 60 W bulb on a mirror (i.e., total reflection) is 400 nN, seven orders of magnitude less than the force exerted by gravity [64]. In experiments on single molecules, forces on the order of 1–10 pN are sufficient to induce deformation. In practice, a large attractive radiation pressure is obtained by the use of high-energy lasers, small (i.e., lightweight) transparent beads, and oil immersion objectives (to maximize the refractive index n and therefore maximize the NA of the objective lenses). Further stabilization of the optical trap can be attained via the use of two opposing, focused lasers (dual beam), such that (repulsive) reflective forces of the lasers cancel out. Despite the increase in trapping force afforded by the dual beam design, its complexity and strict laser alignment requirements make the single beam instrument preferable, especially when beads of relatively large radius ($R \sim 5.0$ µm) are used.

The OT can manipulate relatively large biological samples such as individual cells, as the sample size is determined by the bead diameter (one to several µm sizes are commercially available) or the spot size of the focused laser beam (500 nm or more). A further advantage is that the experimental conditions enable experiments on living cells. The force imposed on cells via OT can be as large as 600 pN (at the present time), with force resolution better than 1 pN. However, as illustrated in the example below, quantitative use of OT requires that the refractive indices of the trapped object (in this example, the attached bead) n_o and surrounding environment n_m be uniform, that $n_o > n_m$, that the biological object be as symmetric as possible, and that the biological object be sufficiently compliant that the laser power P required to deform it will not impart radiation damage. For these reasons, mechanical studies via OT are most applicable to cells located in fluid suspension in vivo, such as blood cells and immune response (T- and B-) cells.

Fig. 9 schematically shows an optical trap apparatus comprising a laser source and an inverted microscope instrumented with a CCD video camera. Beads, coated with ECM protein(s) to enhance cell adhesion, are added to a cell suspension; two such beads are positioned at opposite ends of the cell and given sufficient time to adhere. Note that, as these beads comprise the “grips” by which the cell is manipulated, the adhesion strength of the beads to the cell surface limits the maximum force attainable via this method. It has been shown [66,67] that aspecific binding in this manner facilitates sufficiently large interfacial strength to enable stretching of an erythrocyte to forces as large as 600 pN. In the fluid chamber of the OT apparatus, the position of one cell-attached bead is fixed to a stationary glass slide; this bead acts as the fixed crosshead of a loading frame. The opposing, cell-attached bead is confined via the OT, and its position is modulated via the magnitude of the laser power; this bead acts as the mobile crosshead. An increase in P attracts the bead toward the laser and thus exerts a tensile force on the cell. Chew et al. [66] and Dao et al. [67] employed this particular system to conduct tensile stretch experiments on human erythrocytes, where stretching forces of up to 600 pN and thus strains up to 100% were attained for a 1.5 W (Nd:YAG) laser OT acting on silica beads of 4.1 μm diameter. The relatively high laser power and large bead diameter were capable of producing trapping forces on the cell which were nearly an order of magnitude larger than those achieved previously on whole cells stretched by OT in phosphate buffered saline (PBS) solution [68-70]. Fig. 10 shows an example of the stretching of the whole erythrocyte using the single OT schematically shown in Fig. 9. Here, the geometric changes induced in the cell at several different stretching forces are illustrated by the optical micrographs corresponding to increasing levels of imposed force. Video images of the deformation induced by such tensile stretching can be found in

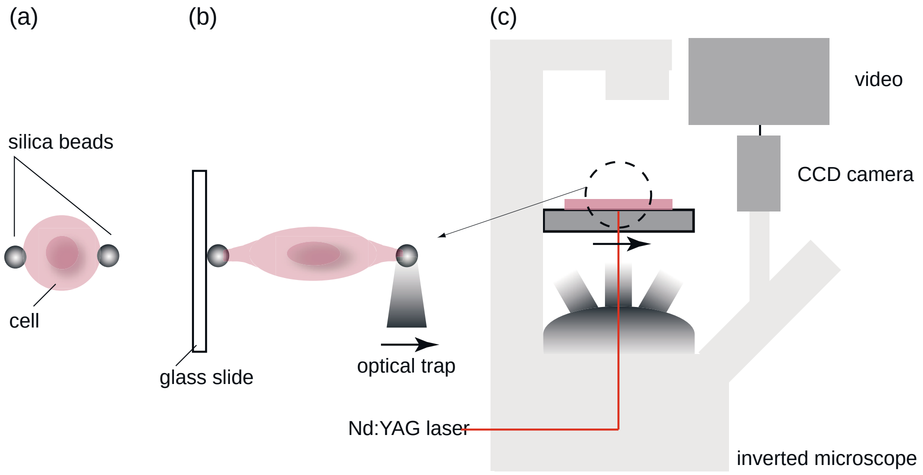

Fig. 9. Schematic showing the arrangement used for the stretching of a cell in a saline solution using the optical tweezers (OT) method. Stretching forces of tens to hundreds of pN can be imposed with this method. (a) Erythrocyte (red blood cell) onto which two diametrically opposed silica beads of 4.1 μm diameter are aspecifically bound via protein coating. (b) Deformation of the erythrocyte via translation of one bead under a moving optical trap. Note that the other bead is fixed to a stationary glass slide (c) Representative experimental apparatus. From Refs. [66, 67].

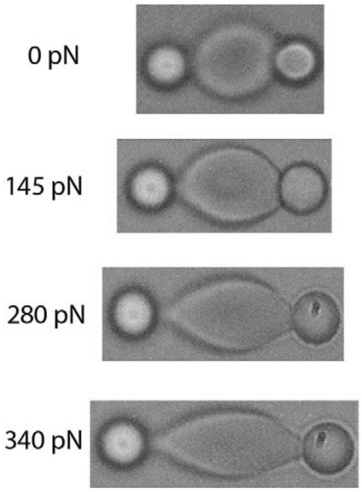

Fig. 10. Optical micrographs showing the deformed geometry of a human red blood cell in a phosphate buffered saline solution at room temperature that is subjected to large deformation in direct tension using optical tweezers (OT). The bead on the right is held fixed to a glass slide while the one on the left is trapped with a laser beam; the displacement of the beam causes the bead to move, thereby stretching the cell. The diameters of the beads is 4.1 μm. From Refs. [66, 67].

the supplementary material archived electronically in [67].

The force calibration procedure for OT is similar to that employed for MTC and magnetic traps (MT), where drag force is calculated as a function of bead displacement in a solution of known viscosity such as glycerol or PBS [66-70]. In OT, the microbead is trapped in PBS at a certain laser power, and a flow chamber imposes increasing shear flow on the bead as the bead is displaced from the OT as a consequence of the drag force F, which is estimated from Stokes' law as:

$$F = 6\pi R\eta_f v \tag{6}$$

where R is the bead radius, η_f is the PBS viscosity, and ν is the velocity of the PBS across the bead. In practice, Eq. (6) must be modified to account for the boundary effects of a closed system. Trapping force can thus be calculated for experiments conducted at the same solution viscosity, known R, and experimentally measured ν. Alternatively, trap stiffness k can be calculated via the power spectral density (frequency dependence of thermal oscillations) of the bead and force F calculated via Eq. (5) for experimentally measured bead displacement x.

In addition to monotonic loading, cyclic and stepwise loading can be imposed via an acousto-optical modulator [69], a standard laser optics control component. Optical tweezers have also been used to impose stretching forces at more than two locations on the cell membrane by proper adhesion of multiple beads at predetermined sites on the cell membrane, in order to approximate loading states such as equibiaxial tension [71], or by multiplication of a single OT via computer generated holograms [72]. This possibility affords considerable flexibility in the control of stress state during the deformation of the entire cell that, in turn, offers a useful experimental tool for probing the constitutive response of the cell membrane. These capabilities point to potential opportunities for establishing molecular level connections between structural changes in the cell and the progression of diseases. Certainly, the nonlinear and non-uniform stress distribution that arises due to the point loading inherent in bead-mediated OT represents a current challenge in the calculation of mechanical parameters.

Due to its high accuracy in force measurement, OT has been used extensively in single-molecule studies [73]. Typically, biomolecules are bound to polystyrene or silica beads (~1 μm in diameter). An optical trap can then be used to steer a bead to interact with a partner molecule attached to a glass coverslip or another bead. Upon binding between the two molecules, the forces and displacements involved can be measured, and the interaction can be perturbed mechanically by moving the trap. Perhaps the most intensive applications of optical tweezers have been studies on the linear motor protein kinesin that transports vesicles and moves along microtubules for up to several μm before dissociating [73]. To characterize the motion of kinesin, Svoboda et al. [74] attached kinesin at low density to silica beads, optically trapped a bead, and moved it near a microtubule that was fixed on a microscope coverslip. The displacement x of kinesin along the microtubule was measured by monitoring the displacement of the bead with nanometer accuracy (Fig. 11(a)). The kinesin molecule was found to move along a microtubule with reg-

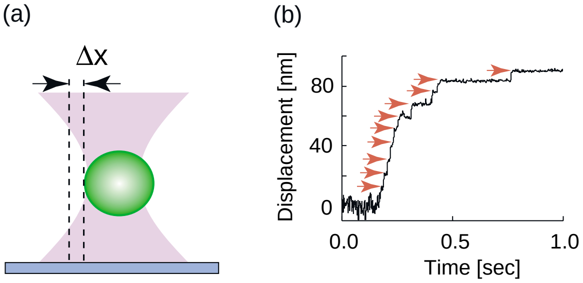

Fig. 11. (a) A single kinesin molecule was attached to a bead trapped by a laser (pink shading). Displacement (Δx) of the kinesin along the microtubule was measured by monitoring the displacement of the bead with nanometer accuracy. (b) Displacement records indicated that the step size (i.e., distance between two sequential red arrows) is 8 nm.

ular 8 nm steps (Fig. 11(b)), coinciding with the periodic spacing of an associated protein ($\alpha\beta$ tubulin dimer), and clearly differentiating from Brownian motion at low adenosine triphosphate (ATP) concentration or at high load. The displacement rate decreased linearly with increasing force over a broad range of ATP concentrations. Using OT, single-molecule studies of kinesin have substantially improved our understanding of how linear molecular motors function and how the mechanical movement is related to the structural features and chemical reactions such as ATP hydrolysis.

3.6. Optical stretcher

An important variation on the OT is termed the optical stretcher (OS), an instrument that obviates the need for synthetic “handles” attached to the cell surface and affords maximum forces of several hundred pN [75]. In the OS, two lasers are shone on diametrically opposite portions of the cell, but are not focused on this plane. This unfocused state reduces the intensity transmitted to the cell, such that high power lasers can be used without damaging the cell; in fact, laser spot size must be greater than the cell diameter for this trap to be stable. Consider the interaction of a single laser with a dielectric object, as shown in Fig. 12(a). When the dielectric object has an index of refraction n_o greater than that of the surrounding medium n_m (as is typical of cells in culture media), the *net* force at the surface point of entry F_e and the *net* force at the surface point of exit F_x are both tensile, oppositely directed, and oriented normal to the surface of the object. The small difference in magnitude of these forces is the scattering force. When a second, diametrically opposed laser is shone on the object, the net stretching force F_s at each entry/exit point is the sum of F_e from one laser and F_x of the other:

$$F_s = F_{1,e} + F_{2,x} = \{[n_m - (1-R)n_c + Rn_m][P/c] + [n_c - (1-R)n_m + Rn_c][(1-R)P/c]\} \quad (7)$$

where n_m and n_o are the refractive indices of the surrounding media and cell, respectively, R is the fraction of reflected light, c is the speed of light in vacuum, and P is total light power. By positioning two divergent lasers opposite one another, the scattering forces cancel at the center of the object and the net stretching forces at the surface double in magnitude, attaining stresses that are approximately 500 times greater than (and forces at least 4 times greater than) those of the OT for the same laser light intensity, e.g., $F_{max} = 400$ pN for a 500 mW laser in aqueous media and can exceed 1 nN [11,76,77]. Further, as the laser beams are necessarily unfocused on the cell, radiation damage is reduced relative to OT. As in OT, stepwise and cyclic loading can be achieved via acousto-optical modulation. Displacement of the cell is measured directly via image analysis, and the corresponding force is calculated via geometric ray optics as a function of the indices of refraction, fraction and direction of light reflected, and total light power [62]. Displacement is limited only by the maximum force attainable via OS, and displace-

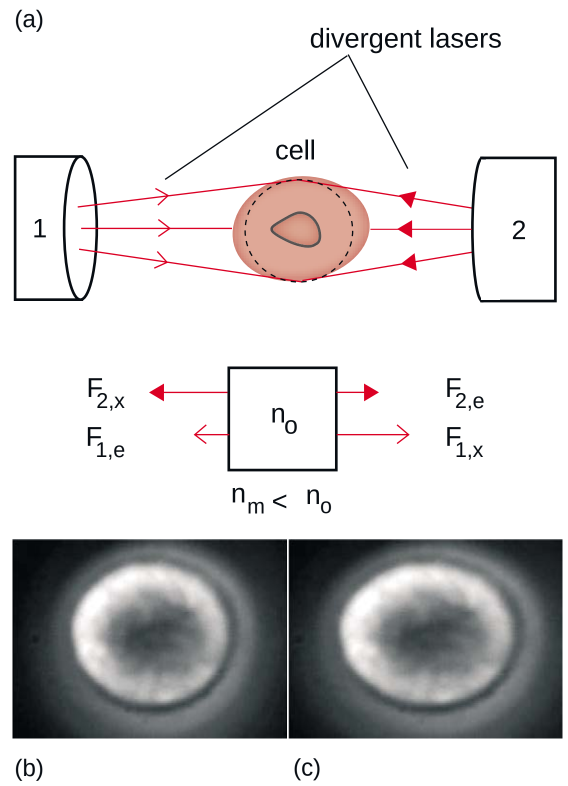

Fig. 12. Optical stretcher (OS) for noncontact single cell studies. (a) Schematic of operating principles. An unfocused laser exerts net tensile forces due to refraction when a laser beam enters Fe and exits Fx the cell surface. The total stretching force Fs due to diametrically opposed lasers is the sum of the net tensile force of exit from one laser (e.g., F1,e) and the net tensile force of entry from the other laser (e.g., F2,x). In order to use ray optics to calculate these forces, it is necessary that the biological object be fairly symmetric, that the refractive indices of the object no and of the surrounding media nm be spatially uniform, and that nm $<$ no. (b) Neutrophil (white blood cell) in optical trap of 150 mW laser power; (c) Uniaxial, noncontact stretching of this neutrophil via 1.1 W laser power. Photographs courtesy of J. Guck and J. Kas.

ment resolution is dependent on the signal/noise ratio of the position analysis method (e.g., measurement via standard optical image tracking of a single point implies resolution on the order of 25 nm, whereas position sensitive photodiodes can yield resolution better than 1 nm). Calculations of force are derived from analytical formulations that are applicable to objects of high symmetry (e.g., spheres), and uniform optical density (e.g., prokaryotic cells). As a result, cells that exhibit anisotropic shape or internal structure, including adherent cells on substrates, are not easily analyzed via this method. Improved analyses of the relevant laser optics that will relax these constraints are in progress [106]. Further, unlike OT, OS is not amenable to single molecule studies.

Note that OS requires that the sample have a greater refractive index than its surrounding media, that n_o is homogeneous across the biological structure, and that the laser intensity does not destabilize the structure. Guck et al. have shown that these requirements are met, and strains of 160% are attainable, for (procaryotic) RBCs and (eucaryotic) PC12 cells and neutrophils [11,75-82], and Moore et al. [82] have shown that OS is sufficiently sensitive to detect changes in the deformability of cells as a function of cancer progression. As shown in Figs. 12(b) and (c), OS imposes sufficiently large, uniaxial strains to deform eucaryotic cells with extensive and dynamic cytosekeletal protein networks, such as neutrophils. Further application of this approach may include high frequency (kHz) mechanical oscillation of mechanosensory cells, as well as flow-assisted cell sorting based on disease-related changes in mechanical stiffness [106].

3.7. *Magnetic traps*

A further variation on the OT is a magnetic trap or tweezers (MT) [83,84]. Here, magnetic beads (250 nm to 5 μm in diameter) serve as “grips” which, under electromagnetic field gradients that impose a local magnetic force on these beads, impose displacement. These beads can be attached through ligand-specific or aspecific binding to a cell surface for single cell studies [23,25,26], or attached through specific chemical functionalization to one end of nucleic acids [83,84] or biomolecules [85] that are fixed at the other end to a rigid surface. The magnitude of the force is controlled directly by and calibrated according to field intensity (i.e., electromagnetic coil current), and the bead position is maintained in a feedback loop with real-time image analysis, effectively trapping the bead in a potential well. Two advantages of this approach over OT are that out-of-plane rotations and thus torque can be considered (as the magnetic field contains an angular component), and that the potential damage to the cell via radiation is eliminated. Currently, the vertical forces attained by MT are of the highest resolution currently available (10 fN), making it possible to conduct elegant experiments at the single molecule level, as shown in Fig. 13. However, due to the requirement of real-time image analysis to measure and control bead displacement, the present stiffness of the MT is two orders of magnitude smaller than that of the OT, the maximum vertical/horizontal forces that can be imposed are on the order of 10 pN–at least an order of magnitude smaller than those achievable via OT and OS. A further limitation of MT is that the magnetic susceptibility of these particles varies widely, such that these experiments can be difficult to calibrate accurately and to control precisely [47]. Although the forces attainable via MT are presently insufficient to deform entire cells, Bausch et al. [23,25] have used MT extensively to measure viscoleastic deformation of portions of living cells and cell membranes.

3.8. Microneedle

The microneedle (MN) technique is one of the earliest experimental approaches developed, whereby portions of the cell are deformed via a cantilevered probe and displacement is measured via optical images [20,21]. Here, the cantilever stiffness k is calibrated experimentally. Maximum force is limited by k and force resolution is limited by optically obtained displacement resolution. As glass microneedles can be drawn to smaller diameters than other fabricated cantilevers, MN is among the softest mechanical cantilever approaches. Force maxima are on the order of 200 pN, with force resolution of 0.6 pN, and displacement maxima are on the order of μm. Thus, this technique can be used to deform whole, adherent cells as well as single molecules. Hwang and Waugh [86] have used MN to semi-quantitatively measure the adhesion between the membrane and actin-rich cortex of an erythrocyte, and Ishijima et al. [87] were among the first to measure actin-actin monomer binding via MN.

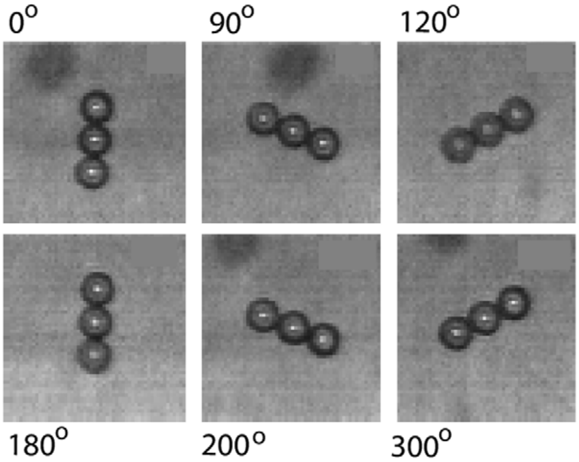

Fig. 13. Magnetic tweezers (MT) for single molecule studies. DNA strands uncoil under the applied torque of the magnetic bead assembly. Such experiments allow one to measure fN - level forces. Reprinted with permission from the American Association for the Advancement of Science, Ref. [84].

The cytodetacher (CD) is a modification of MN that provides a means to investigate the adhesion of cells to various substrates [8]. This instrument applies a concentrated mechanical force normal to the cell/substrate interface (i.e., shear force) via a cantilevered probe (Fig. 14). The deflection of this probe x is monitored within an inverted optical microscope via a position-sensitive photodiode, and force F is calculated directly from this deflection according to the elastic beam relation in Eq. (3). Substrates of various composition are deposited on the edge of glass slides, and cells are subsequently seeded on these substrates. After a specified duration of culture, the attached cell is displaced via the cantilevered probe (e.g., over a distance of 10 μm and a displacement rate of 1 μm/s). The force F required to detach the cell from the substrate is considered equal to the attachment force of adhesion. Although this method provides a means to compare qualitatively the adhesion between a cell and a given substrate, the complex shear stress state and relatively large size of the cantilevered probe (with respect to the cell diameter) makes quantitative analysis of the forces, stresses and mechanisms of adhesion quite complex. Further, the total adhesion force measured by CD cannot be related quantitatively to the individual force contributions of the FACs that are known to be the points of contact between the cell and the substrate because the number of these FACs in

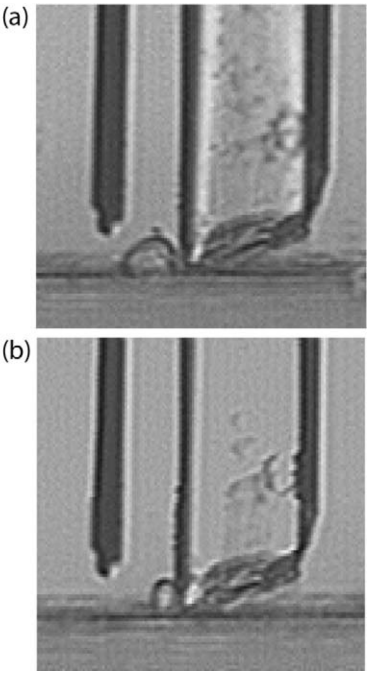

Fig. 14. Cytodetacher (CD) for single cell studies. A modification of the microneedle (MN). The individual cell is approached by the CD probe in (a) and is detached from the substratum in (b). Displacment of the MN can be measured via deflection of the parallel carbon fiber, as recorded via a position sensitive photodiode. Images courtesy of C.C. Scott and K. Athanasiou.

each cell and the unit force of a (multimolecular) FAC rupture event are not known.

3.9. Atomic force microscopy and force spectroscopy

Atomic force microscopy (AFM) is a specific example of scanning probe microscopy, and was an adaptation of a scanning tunneling microscope that formed images through tunneling current between a probe and a conductive sample [88]. In AFM, the images are not generated via reflection or transmission of photons or electrons, but rather are created via local application of mechanical force across a sample surface in one or more spatial dimensions. In the most typical AFM configuration (Fig. 15), force (10^{-12}–10^{-8} N) is applied to the sample surface through a sharp (nm-scale radius) tip positioned normal to the free end of a flexible Si-based cantilever. The relative displacement of this tip x is tracked via a laser that reflects off of the back surface of the cantilever onto a position sensitive photodiode, a device that converts laser light to voltage V. The voltage is converted to displacement by determining $V(x)$ experimentally: While measuring V, a calibrated displacement transducer actuates the cantilever base until the cantilever tip contacts against a rigid surface, such that the tip displacement is equal in magnitude (but opposite in direction) to that of the transducer.

Through feedback with the cantilever base transducer, contact mode AFM imaging is attained by maintaining $V(x)$—and thus tip deflection and contact force—at a fixed value as the cantilever tip scans the sample surface. The resulting displacement of the cantilever base comprises the height map, or gross (nm to μm-scale) features of the surface topography. Since this electronic feedback is not ideal, there are small differences between the desired and the actual tip deflection that comprise an additional image (the error signal image). This image quantifies nm-scale surface topography that can be superposed on the height image. Tip deflection is converted to force F via Eq. (1), where the cantilever stiffness k_c is calibrated independently via deflection of the cantilever against a rigid substrate (e.g., glass) or via the equipartition theorem for a simple harmonic oscillator:

$$[1/2]k_BT = E_{avg} = [1/2]k_c\sqrt{<x^2>} \tag{8}$$

where k_c is the cantilever spring constant and $\sqrt{\langle x^2\rangle}$ is the root mean square cantilever tip displacement. Alternatively, the cantilever can be oscillated above the surface such that it intermittently approaches and/or contacts the sample (tapping mode). Thus, voltage-derived forces generate images corresponding to parameters such as sample height, charge density, or intermolecular forces depending on the operational mode of the AFM. The resulting image quantifies both the surface topography and the relative stiffness of sample regions.

AFM has been exploited as a research tool by the biophysics community because this technique affords Angstrom-scale positioning accuracy, the ability to both image and mechanically manipulate

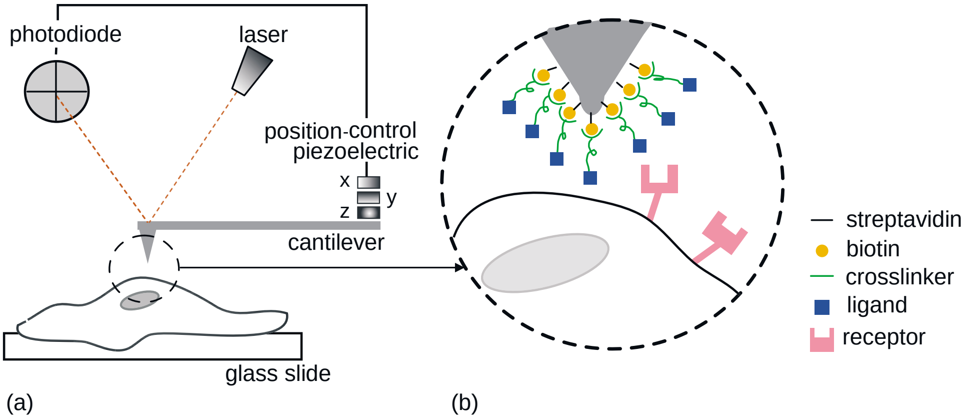

Fig. 15. Schematic of atomic force microscope (AFM). (a) Mechanical contact is controlled via feedback between a piezo-actuated cantliever base and a photodiode that measures cantilever tip deflection signals. (b) Chemical functionalization of this tip can enable molecule-specific interations on controlled molecular surfaces or on cells. Force-deflection experiments that quantify such surface interactions are termed high resolution force microscopy (HRFS)..

a single biological structure with better than nm/pN resolution (Fig. 16(a)), and the potential to track biological processes in near physiological environments over time. Here, it is important to note that, due to the contact-based nature of AFM, its use in cell mechanics is restricted to cells that can adhere tightly to a substrate over the course of an experiment. This method is related to the microneedle (MN) technique whereby portions of the cell are deformed via a cantilevered probe and deformation is measured via optical images, but in contrast high resolution images of the deformed structure can be obtained, and high resolution force-displacement data can be recorded continuously during deformation. In this way, MN is related to AFM in the same way that hardness testing is related to instrumented indentation.

The spring constant k_c of the AFM cantilever determines the maximum force attainable, and the thermal fluctuations of the cantilever determine the resolution of the instrument. Note that the signal to noise ratio does not improve as k_c decreases, such that softer cantilevers do not provide increased force resolution. As different geometries and base materials are readily available, k_c can range from 0.003–10 N/m, such that pN-scale forces and nm-scale deflections are attainable. As shown in Fig. 16 and previously by others [13,16,17,89-93], the contact-based, force-controlled image indicates the structure of subsurface elements because the cytoskeleton confined beneath the cell surface is more stiff than the overlying cell membrane. Thus, despite the limitation that such error signal images do not accurately reflect the true height distribution of the cell, such contact imaging allows the systematic manipulation of these important cellular components. Fluorescent labeling and chemical disruption of the cytoskeletal proteins [17] have been used in concert with AFM to show that actin filaments contribute more to the mechanical stiffness of the cell than do microtubules, despite the fact that microtubules are of greater diameter.

Extensions of these AFM capabilities include the culture of living cells on the AFM tip to study cell-cell and cell-substrate adhesion [18] and chemical functionalization of the AFM tip to facilitate chemomechanical interaction with cell surface receptors [94]. This functionalization is specific to the cantilever material and molecule of interest, and is obtained through sequential solution immersions such that the molecule of interest is strongly bound to and exposed far from the tip. In fact, by promoting adhesion between the cantilever tip and the sample surface, subsequent retraction of the tip can induce pN- to nN-scale tensile forces on specific surface features including individual cell surface molecules, a technique termed high resolution force spectroscopy (HRFS). As shown in Fig. 16(c) and (*d*) for a model ligand-receptor system (biotin-

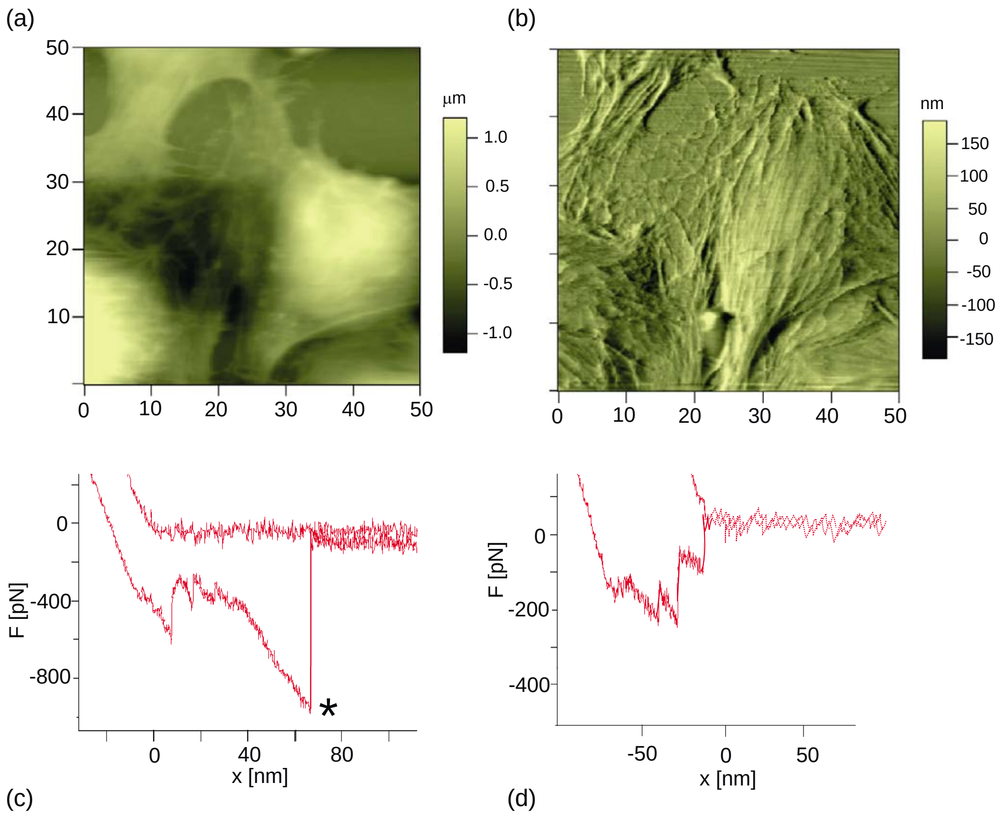

Fig. 16. Atomic force microscopy and force spectroscopy for single cell and single molecule studies. (a) Height image of bovine capillary endothelial cells on gelatin substrate; (b) Deflection (feedback error) image of these cells show cytoskeletal detail; (c) Specific ligand-receptor rupture event (∗) for streptavidin substrate and biotin-functionalized cantilever tip; (d) Aspecific binding for clean glass surface and biotin-functionalized cantilever tip. Images courtesy of A. Chandrasekaran and K.J. Van Vliet. All images and data were acquired via the MFP3D (Asylum Research, Santa Barbera, CA) instrumented with a Si_3N_4 cantilever.

streptavidin), HRFS with a chemically functionalized tip can be used to determine the unbinding force between molecules of interest, estimate molecular length, and explore the kinetics of molecular interactions as a function of chemical and mechanical environments. For example, AFM and HRFS of proteoglycan macromolecules have been implemented jointly to understand the unique mechanical toughness of human cartilage in vitro [95,96].

In particular, AFM has been used to explore the elastic deformation of cells and cellular components such as the cytoskeleton. A thorough review of such experiments is given by Radmacher [13]. For example, the elastic behavior of the cytoskeletal filaments can be explored via AFM as a function of position with the cell, first by creating a contact-based image (Fig. 16(a) and (b)) of the cell and then by conducting high resolution force spectroscopy (HRFS) measurements at particular points on that image (here, contact loading akin to nanoindentation). If progress can be made to convert the important qualitative findings and force-displacement data obtained via AFM into quantitative measurements of useful mechanical parameters, this approach can be used to probe the role and mechanical properties of these cytoskeletal components—data upon which many analytical and computational modeling efforts rely. At present, this effort is limited by several important distinctions between the contact imposed via AFM and that assumed in the established analysis of nanoscale contact deformation (nanoindentation). First, due to the use of a laser for positional tracking, the cantilever is inclined at an angle to the surface (15°), such that the tip (a four-sided pyramid with an included apex angle of 35° and radius on the order of 20 nm) does not approach normal to the cell surface. As such, the indentation geometry is no longer self-similar, and loading contains a strong lateral force component (frictional stresses between the tip and the sample). Further, although the elastic theories of Hertz and Sneddon [97] are often applied in the analysis of these data, both of these classic approaches are applicable to normal contact and time-independent, linear elastic half spaces. These assumptions are not valid for deformation of living cells adhered to a substrate, effectively acting as (layered) thin films on a substrate. There is significant effort underway within the biophysics community to address these limitations, and increased interaction between the mechanical and materials engineering communities who have made significant progress in the analysis and interpretation of contact-based experiments may lead to more rapid maturation of this important tool.

AFM can also be utilized to study single-molecule biomechanics, including the unbinding of antibody-antigen, ligand-receptor, and DNA-protein pairs [98]. The experimental set up for unbinding of a ligand-receptor pair is similar to that shown schematically in Fig. 15(a), except that the receptor molecules are adsorbed on a glass surface instead of expressed on a cell membrane [99]. When the AFM tip contacts the chemically functionalized surface, binding occurs between the ligand and receptor. Upon retraction of the cantilever, the bonds between the receptor and ligand may break, resulting in the unbinding of the two molecules. The corresponding unbinding force can be calculated from the deflection of the cantilever at rupture. For example, using AFM, the rupture force and lifetime of the P-selectin and PSGL-1 (P-selectin glycoprotein ligand-1) complex were measured. The AFM tip was functionalized with PSGL-1 by first adsorbing onto the tip a monoclonal antibody specific for that protein (anti-PSGL-1 mAb PL2), and then blocking aspecific binding of other species with another protein (1% bovine serum albumin, or BSA). P-selectin was reconstituted in a PEI (polyethylenimine) polymer-supported lipid bilayer. Binding between P-selectin and PSGL-1 was realized when the tip was brought to contact with the bilayer for 3 s with a ~20 pN compressive force. The cantilever was then retracted at a displacement rate of 250 nm/s, and then maintained at a fixed deflection to apply a constant force to the bond(s). The bond lifetime was measured from the instant when the cantilever deflection was halted to the instant of bond(s) failure. It was demonstrated that binding between certain ligand-receptor pairs may have both catch bond and slip bond behavior. That is, increasing force first prolonged and then shortened the lifetime of the receptor-ligand complex [99]. This dual response to force provides a mechanism to regulate cell adhesion under variable mechanical force.

There are several important issues in unbinding force measurement. First, for single-molecule studies, it is necessary to ensure that only one ligand-receptor pair is formed and ruptured, so that the rupture force measured truly reflects the interaction between a single molecular pair. Second, the rupture force is usually dependent on the loading rate, especially for weak noncovalent bonds. Finally, the cantilever has on average a thermal energy of 0.5 k_BT, which implies that the smallest force that can be accurately measured using commercially available silicon nitride cantilever is on the order of ~10 pN. For relatively weak interactions between biomolecules, with an equivalent rupture force of $\leq$10 pN, OT (Section 3.4) offers a viable alternative for force measurement.

3.10. Biomembrane force probe

Finally, a technique related to MA but developed for single molecule experiments is the biomembrane force probe (BFP), whereby a cell or lipid vesicle is partially aspirated in a micropipette and then serves as the force transducer. As shown in Fig. 17, ligand-coated beads are attached to this pressurized capsule and positioned to interact with a receptor of interest that is adhered to a nearby substrate. Deformation of the capsule is measured optically, and force maxima are controlled by the surface tension (i.e., aspiration pressure) imposed

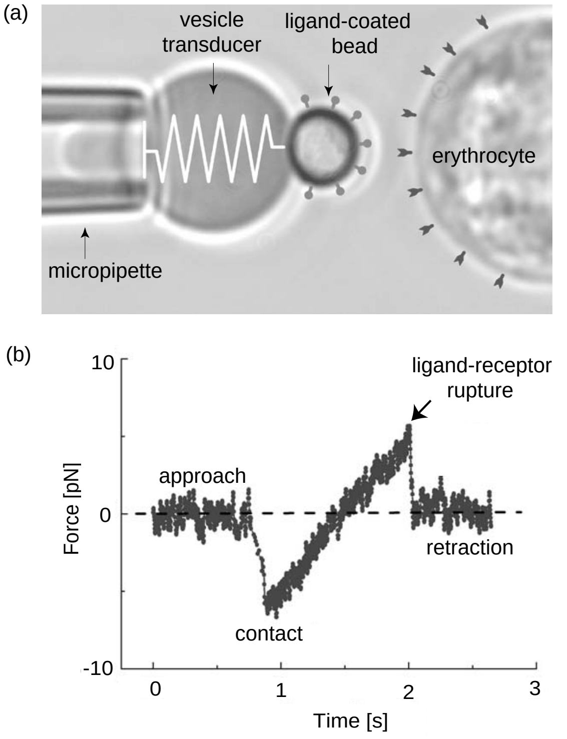

Fig. 17. Biomembrane force probe (BFP) for single molecule studies. (a) The vesicle acts as a force transducer, relating the interaction forces between a ligand-coated polystyrene bead and the cell-surface receptors of an erythrocyte. (b) The ligand-receptor binding/unbinding forces measured depend on the rate of loading/unloading. This symmetric, low force response is typical of slow rates (10 pN/s). Images courtesy of E. Evans.

on this capsule. Force maxima approach 1000 pN, with resolution of 0.5 pN, and displacement resolution is on the order of 500 nm. An interesting example of this approach is shown in Fig. 17(a), where erythrocyte-ECM adhesion was probed directly by using the erythrocyte as the force transducer [9].

This BFP method has also been utilized to illustrate the loading-rate dependence of the ligand-receptor unbinding force (Fig. 17b) [100]. In particular, using BFP, the bond strength of the streptavidin (or avidin)-biotin complex was found to increase from about 5 to 170 pN when loading rate increased over six orders of magnitude [101], as shown in Fig. 18. Therefore, binding between two proteins may appear strong or weak depending on loading rate. In this experiment, amino silane groups were covalently bound to glass microbeads. Amine-reactive polyethylene glycol (PEG) polymers with and without biotin end groups were covalently linked to the silanized surfaces, and the biotinylated beads were exposed to excess (strept)avidin and then washed. An erythrocyte covalently linked with PEG-biotin polymers was joined to the avidinated microbead to construct the probe, similar to Fig. 17(a). Although the BFP

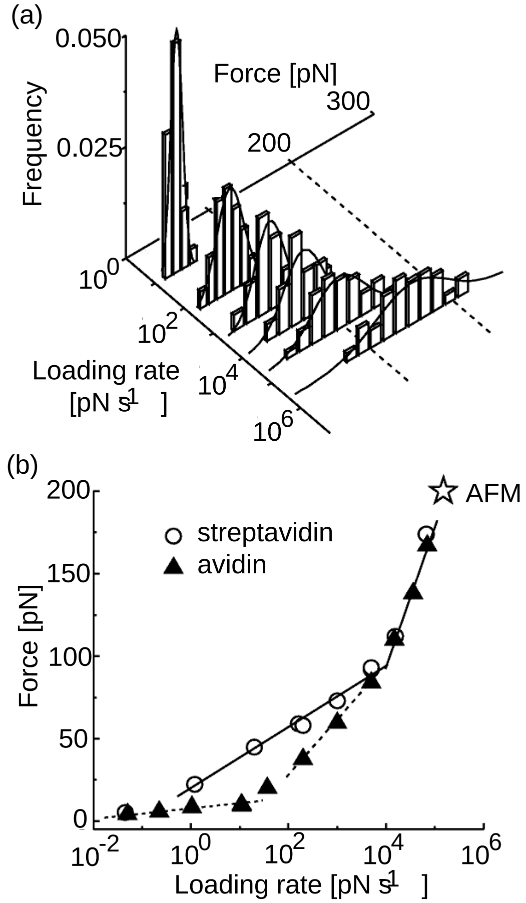

Fig. 18. Biotin–streptavidin bond strengths measured via BFP. (a) Force histograms from BFP experiments on single biotin–streptavidin bonds demonstrate shift in peak location and increase in width with increase in loading rate. Gaussian fits used to determine the most frequent rupture force or bond strength are shown. (b) Dynamic strength spectra for biotin–streptavidin (circles) and biotin-avidin (triangles) bonds. Consistent with the high-strength regime is the biotin–streptavidin strength measured recently by atomic-force microscopy (AFM).

method is quite specialized and does not provide force or displacement capabilities distinct from those achievable via the other techniques discussed herein, BFP remains an interesting example of how cell mechanics may be exploited in instrument design for single molecule biomechanics studies.

4. Concluding remarks

In this review, we have outlined an impressive array of experimental tools that can be utilized to further our understanding of whether and how the mechanical environment and mechanical behavior of a cell affects its biological function. Despite the apparent simplicity of the force-displacement relationships that govern these techniques, the sophistication of our experimental tools far exceeds our current analytical and computational understanding. Rigorous interpretations of how force, stress and energy can be imposed and measured via these approaches will enable more accurate assessment of current results and also more lucid comparison of results among the different experimental tools. Certainly, the coupled chemical interactions and the inherent time dependence of molecular and cellular processes present challenging opportunities for further research (see, e.g., Ref. [102]). Further, in order to maximize the engineering potential of these capabilities, it is essential to recognize how biological systems are intrinsically different from synthetic material systems, as well as which outstanding questions in developmental and pathological biology can be addressed via quantification of mechanical responses.

For example, it is interesting to note that the mechanical response of individual cells and cell membranes is known to have a direct connection to certain pathologies. Recent experiments performed using OT [60] and MA [103] have shown that infestation of human erythrocytes with the malaria parasite *plasmodium falciparum* can cause up to a ten fold increase in the cell membrane shear modulus as the disease state progresses. The interaction of parasite proteins with the cell cytoplasm, actin cortex and other membrane components mediates structural and functional changes of the erythrocyte which, in turn, are reflected in the mechanics of deformation of the cell [104]. How such connections can be used to probe the specific mechanisms by which different diseases progress and the means by which they can be diagnosed and treated effectively remain topics of considerable opportunity and challenge in which the biomechanics tools considered in this review article will inevitably play a critical role. Our collective and sustained interaction with experts from other established research communities including cell and molecular biology and biophysics can serve to clarify the mechanical concepts relevant to disease and development, and to increase our own understanding of how the fundamental mechanics and physics of material systems are affected by environmental interactions.

Acknowledgements

The authors gratefully acknowledge those who contributed images and helpful discussion on specific techniques, especially Y.-L. Wang, J. Guck, J. Kas, F. Guilak, J. Tan, C. Chen, E. Evans, C.C. Scott, K. Athanasiou and A. Gouldstone. KJVV thanks M.A. Moses at Children's Hospital Boston, Harvard Medical School, and the Department of Materials Science and Engineering at MIT for financial support. SS acknowledges support for the preparation of this paper from the US Army Research Office and from the Singapore-MIT Alliance. GB acknowledges the support of the US Army Research Office (grant No. 44062-EG).

References

[1] Feeback DL, Clarke MSF. Improved unidirectional cell-stretching device. In: Book Improved unidirectional cell-stretching device. http://www.nasatech.com/Briefs/Aug00/MSC22834.html; 2000.

[2] Pelham RJ, Wang Y-L. Cell locomotion and focal adhesions are regulated by substrate flexibility. Proceedings of the National Academy of Science USA 1997;94:13661–5.

[3] Beningo KA, Wang Y-L. Flexible substrata for the detection of cellular traction forces. Trends in Cell Biology 2002;12:79–84.

[4] Tan JL, Tien J, Pirone DM, Gray DS, Bhadriraju K, Chen CS. Cells lying on a bed of microneedles: An approach to isolate mechanical force. Proceedings of the National Academy of Science 2003;100:1484–9.

[5] Fabry B, Butler JP, Navajas D, Tschumperlin DJ, Laporte JD, Maksym GN, Fredberg JJ. Mechanical properties of cultured human airway smooth muscle cells from 0.05 to 4 Hz. J Appl Physiol 2000;89.

[6] Puig-de-Morales M, Grabulosa M, Alcaraz J, Mullol J, Maksym GN, Fredberg JJ, Navajas D. Measurement of cell microrheology by magnetic twisting cytometry with frequency domain demodulation. Journal of Applied Physiology 2001;91:1152–9.

[7] Maksym GN, Fabry B, Butler JP, Navajas D, Tschumperlin DJ, Laporte JD, Fredberg JJ. Mechanical properties of cultured human airway smooth muscle cells from 0.05 to 0.4 Hz. Journal of Applied Physiology 2000;89:1619–32.

[8] Athanasiou KA, Thoma BS, Lanctot DR, Shin D, Agrawal CM, LeBaron RG. Development of the cytodetachment technique to quantify mechanical adhesiveness of the single cell. Biomaterials 1999;20:2405–15.

[9] Yeung A, Evans E. Cortical shell-liquid core model for passive flow of liquid-like spherical cells into micropipets. Biophysical Journal 1989;56:139–49.

[10] Evans E, Yeung A. Apparent viscosity and cortical tension of blood granulocytes determined by micropipet aspiration. Biophysical Journal 1989;56:151–60.

[11] Ananthakrishnan R, Moon TJ, Cunningham CC, Guck KJJ. Optical deformability of soft biological dielectrics. Physical Review Letters 2000;84:5451–4.

[12] Wu HW, Kuhn T, Moy VT. Mechanical properties of l929 cells measured by atomic force microscopy: Effects of anticytoskeletal drugs and membrane crosslinking. Scanning 1998;20:389–97.

[13] Radmacher M. Measuring the elastic properties of living cells by the atomic force microscope. Atomic Force Microscopy in Cell Biology 2002;68:67–90.

[14] Czajkowsky DM, Shao ZF. Supported lipid bilayers as effective substrates for atomic force microscopy. Atomic Force Microscopy in Cell Biology 2002;68:231–41.

[15] Goldmann WH. Mechanical manipulation of animal cells: cell indentation. Biotechnology Letters 2000;22:431–5.

[16] Rotsch C, Braet F, Wisse E, Radmacher M. AFM imaging and elasticity measurements on living rat liver macrophages. Cell Biol Int 1997;21:685–96.

[17] Rotsch C, Radmacher M. Drug induced changes in cytoskeletal structure and mechanics in fibroblasts-An atomic force microscopy study. Biophysical Journal 2000;78:520–35.

[18] Benoit M. Cell adhesion measured by force spectroscopy on living cells. Atomic Force Microscopy in Cell Biology 2002;68:91–114.

[19] Chen AL, Moy VT. Single-molecule force measurements. Atomic Force Microscopy in Cell Biology 2002;68:301–9.

[20] Felder S, Elson EL. Mechanics of fibroblast locomotion: Quantitative analysis of forces and motions at the leading lamellas of fibroblasts. Journal of Cell Biology 1990;111:2513–26.

[21] Peterson NO, McConnaughey WB, Elson EL. Dependence of locally measured cellular deformability on position in the cell, temperature and cytochalasin B. Proceedings of the National Academy of Sciences USA 1982;79:5327–31.

[22] Sleep J, Wilson D, Simmons R, Gratzer W. Elasticity of the red cell membrane and its relation to hemolytic disorders: An optical tweezers study. Biophysical Journal 1999;77:3085–95.

[23] Bausch AR, Ziemann F, Boubitch AA, Jacobson K, Sackmann E. Local measurements of viscoelastic parameters of adherent cell surfaces by magnetic bead rheometry. Biophysical Journal 1998;75:2038–49.

[24] Crick FHC, Hughes AFW. The physical properties of the cytoplasm. a study by the means of the magnetic particle method. Experimental Cell Research 1965;1:37–80.

[25] Bausch AR, Moller W, Sackmann E. Measurement of local viscoelasticity and forces in living cells by magnetic tweezers. Biophysical Journal 1999;76:573–9.

[26] Alenghat FJ, Fabry B, Tsai KY, Goldmann WH, Ingber DE. Analysis of cell mechanics in single vinculin-deficient cells using a magnetic tweezer. Biochemical and Biophysical Research Communications 2000;277:93–9.

[27] Brown TD. Techniques for mechanical stimulation of cells in vitro: A review. Journal of Biomechanics 2000;33:3–14.

[28] Pioletti DP, Muller J, Rakotomanana LR, Corbeil J, Wild E. Effect of micromechanical stimulations on osteoblasts: development of a device simulating the mechanical situation at the bone-implant interface. Journal of Biomechanics 2003;36:131–5.

[29] Lee AA, Delhaas T, Waldman LK, MacKenna DA, Villarreal FJ, McCulloch AD. An equibiaxial strain system for cultured cells. American Journal of Physiology-Cell Physiology 1996;40:C1400–C8.

[30] Zhu C, Bao G, Wang N. Cell mechanics: Mechanical response, cell adhesion, and molecular deformation. Annual Review of Biomedical Engineering 2000;2:189–226.

[31] Jones DB, Nolte H, Scholubbers GE, Turner J, Veltel D. Biochemical signal transduction of mechanical strain in oseoblast-like cells. Biomaterials 1991;12:101–10.

[32] Dunn A, Moses MA, Van Vliet KJ. Effects of radial, cyclic strain on enzyme activity in endothelial cells 2003 (in preparation).

[33] Wang HC, Ip W, Boissy R, Grood ES. Cell orientation response to cyclically deformed substrates: Experimental validation of a cell model. Journal of Biomechanics 1543;1995:28.

[34] Pfister BJ, Weihs TP, Betenbaugh M, Bao G. An in vitro uniaxial stretch model for axonal injury. Ann Biomed Eng 2003;31:589–98.

[35] Cohen Y, Ramon O, Kopelman IJ, Mizrahi S. Journal of Polymer Science B 1992;30:1055-1067.
[36] Lo C-M, Wang H-B, Dembo M, Wang Y-L. Cell movement is guided by the rigidity of the substrates. Biophys J 2000;79:144–52.
[37] Lo C-M, Wang H-B, Dembo M, Wang YL. http://ylwang.umassmed.edu/video/guidance.htm, City 2000.
[38] Wang N, Ostuni E, Whitesides GM, Ingber DE. Micropatterning tractional forces in living cells. Cell Motility and the Cytoskeleton 2002;52:97–106.
[39] Munevar S, Dembo M, Wang Y-L. Traction force microscopy of normal and transformed fibroblasts. Biophys J 2001;80:1744–57.
[40] Butler JP, Wang N, Ingber DE. Mechanotransduction across the cell surface and through the cytoskeleton. Science 1993;260:124–1127.
[41] Fabry B, Maksym GN, Hubmayr RD, Butler JP, Fredberg JJ. Implications of heterogeneous bead behavior on cell mechanical properties measured with magnetic twisting cytometry. Journal of Magnetism and Magnetic Materials 1999;194:120–5.
[42] Dike LE, Chen CS, Mrksich M, Tien J, Whitesides GM, Ingber DE. Geometric control of switching between growth, apoptosis, and differentiation during angiogenesis using micropattened substrates. In vitro Cell Dev Biol 1999;35:441–8.
[43] Parker KK, Brock AL, Brangwynne C, Mannix RJ, Wang N, Ostuni E, Geisse NA, Adams JC, Whitesides GM, Ingber DE. Directional control of lamellipodia extension by constraining cell shape and orienting cell tractional forces. FASEB 2002;16:1195–204.
[44] Singhvi R, Kumar A, Lopez GP, Stephanopoulos GN, Wang DIC, Whitesides GM, Ingber DE. Engineering cell shape and function. Science 1994;264:696–9.
[45] Xia Y, Whitesides GM. Soft lithography. Ann Rev Mater Sci 1998;28:153–84.
[46] Hochmuth RM. Micropipette aspiration of living cells. Journal of Biomechanics 2000;33:15–22.
[47] Shao J-Y. Measuring piconewton forces and its application in cellular and molecular biomechanics. Advances in Biomechanics 2001:47-51.
[48] Hochmuth RM, Ting-Beall HB, Beaty BB, Needham D, Tran-Son-Tay R. Viscosity of passive human neutrophils undergoing small deformations. Biophysical Journal 1993;64:1596–601.
[49] Sato J, Levesque MJ, Nerem RM. Micropipette aspiration of cultured bovine aortic endothelial cells exposed to shear stress. Arteriosclerosis 1987;7:276–86.
[50] Jones WR, Ting-Beall HP, Lee GM, Kelley SS, Hochmuth RM, Guilak F. Alterations in the Young's modulus and volumetric properties of chondrocytes isolated from normal and osteoarthritic human cartilage. Journal of Biomechanics 1999;32:119–27.
[51] Secomb TW. Red-blood-cell mechanics and capillary blood rheology. Cell Biophysics 1991;18:231–51.
[52] Secomb TW, Hsu R. Red blood cell mechanics and functional capillary density. International Journal of Microcirculation-Clinical and Experimental 1995;15:250–4.
[53] Wu JZ, Herzog W, Epstein M. Modelling of location- and time-dependent deformation of chondrocytes during cartilage loading. Journal of Biomechanics 1999;32:563–72.
[54] Wu JZ, Herzog W. Finite element simulation of location- and time-dependent mechanical behavior of chondrocytes in unconfined compression tests. Annals of Biomedical Engineering 2000;28:318–30.
[55] Guilak F, Mow VC. The mechanical environment of the chondrocyte: a biphasic finite element model of cell-matrix interactions in articular cartilage. Journal of Biomechanics 2000;33:1663–73.
[56] Haider MA, Guilak F. An axisymmetric boundary integral model for incompressible linear viscoelasticity: Application to the micropipette aspiration contact problem. Journal of Biomechanical Engineering-Transactions of the ASME 2000;122:236–44.
[57] Haider MA, Guilak F. An axisymmetric boundary integral model for assessing elastic cell properties in the micropipette aspiration contact problem. Journal of Biomechanical Engineering-Transactions of the ASME 2002;124:586–95.
[58] Boey SK, Boal DH, Discher DE. Biophysical Journal 1998;75:1573-1583.
[59] Discher DE, Boad DH, Boey SK. Biophysical Journal 1998;75:1584-1597.
[60] Lim CT, Lee YS, Tan K, Dao M, Suresh S. National University of Singapore and Massachusetts Institute of Technology. National University of Singapore and Massachusetts Institute of Technology; 2003 (unpulbished results).
[61] Ashkin A. Optical Letters 1986;11:288.
[62] Ashkin A, Dziedzic JM. Optical trapping and manipulation of viruses and bacteria. Science 1987;235:1517–20.
[63] Smith SB, Cui Y, Bustamante C. An optical-trap force transducer that operates by direct measurement of light momentum. Methods in Enzymology 2002;79:144–52.
[64] Williams MC. Optical tweezers: Measuring piconewton forces. In: Schwille P, editor. Single Molecule Techniques. Biophysics Textbook Online; 2002.
[65] Gittes F, Schmidt C. In: L. Wilson, M. Sheetz, P. Matsudaira (Eds.), Laser Tweezers in Cell Biology. San Diego: Academic Press; 1998.
[66] Chew KT, Lim CT, Sow CH, Dao M, Suresh S. Large deformation of human red blood cell by direct stretch using optical tweezers. 2003 (in preparation).
[67] Dao M, Lim CT, Suresh S. Mechanics of the human red blood cell deformed by optical tweezers. J Mech Phys Solids 2003, (in press).
[68] Henon S, Lenormand G, Richert A, Gallet F. Biophys J 1999;76:1145-1151.
[69] Sleep J, Wilson D, Simmons R, Gratzer W. Biophys J 1999;77:3085-3095.

[70] Lenormand G, Henon S, Richert A, Gallet F. Biophys J 2001;81:43-56.

[71] Prentiss H. Unpublished discussion of four optical traps to manipulate cells. http://atomsun.harvard.edu/; 2003.

[72] Curtis JE, Koss BA, Grier DG. Dynamic holographic optical tweezers. Opt Comm 2002;207:169–75.

[73] Mehta AD, Rief M, Spudich JA, Smith DA, Simmons RM. Single-molecule biomechanics with optical methods. Science 1999;283:1689–95.

[74] Svoboda K, Block SM, Asbury CL, Shaevitz JW, Lang MJ. Force and velocity measured for single kinesin molecules. Cell 1994;77:773–84.

[75] Guck J, Chiang JA, Kas J. The optical stretcher: A novel tool to characterize the cytoskeleton. Molecular Biology of the Cell 1998;9:609.

[76] Guck J, Ananthakrishnan R, Moon TJ, Cunningham CC, Kas J. Optical deformability of soft biological dielectrics. Physical Review Letters 2000;84:5451–4.

[77] Guck J, Ananthakrishnan R, Moon TJ, Cunningham CC, Kas J. Optical deformability of cells. Biophysical Journal 2000;78:2170Pos.

[78] Guck J, Ananthakrishnan R, Mahmood H, Moon TJ, Cunningham CC, Kas J. The optical stretcher: A novel laser tool to micromanipulate cells. Biophysical Journal 2001;81:767–84.

[79] Guck J, Ananthakrishnan R, Mahmood H, Moon TJ, Cunningham CC, Hallworth R, Kas J. The optical stretcher-A novel laser tool to micromanipulate cells. Biophysical Journal 2001;80:1138.

[80] Guck J, Ananthakrishnan R, Cunningham CC, Kas J. Stretching biological cells with light. Journal of Physics-Condensed Matter 2002;14:4843–56.

[81] Kas J, Guck J, Chiang JA. The optical stretcher - A novel tool to manipulate cells. Biophysical Journal 1999;76:A276–A.

[82] Moore SA, Guck J, Ananthakrishnan R, Cunningham CC, Kas JA. The reverse progression of cancer in HL-60 cells as monitored by optical deformability. Biophysical Journal 1683;2002:82.

[83] Smith SB, Finzi L, Bustamante C. Direct mechanical measurements of the elasticity of single DNA molecules by using magnetic beads. Science 1992;258:1122–6.

[84] Strick TR, Allemand JF, Bensimon D, Bensimon A, Croquette V. The elasticity of a single supercoiled DNA molecule. Science 1996;271:1835–7.

[85] Gosse C, Croquette V. Magnetic tweezers: Micromanipulation and force measurement at the molecular level. Biophysical Journal 2002;82:3314–29.

[86] Hwang WC, Waugh RE. Energy of dissociation of lipid bilayer from the membrane skeleton of red blood cells. Biophysical Journal 1997;72:2669–78.

[87] Ishijima A, Doi T, Sakurada K, Yanagida T. Subpiconewton force fluctuations of actomyosin in vitro. Nature 1991;352:301–6.

[88] Binnig G, Quate CF, Gerber C. Atomic force microscope. Physical Review Letters 1986;56:930–4.

[89] Barbee KA. Changes in surface topography in endothelial monolayers with time at confluence: Influence on subcellular shear stress distribution due to flow. Biochemistry and Cell Biology-Biochimie Et Biologie Cellulaire 1995;73:501–5.

[90] Charras G, Lehenkari P, Horton M. Biotechnological applications of atomic force microscopy. Atomic Force Microscopy in Cell Biology 2002;68:171–91.

[91] Kumar S, Hoh JH. Probing the machinery of intracellular trafficking with the atomic force microscope. Traffic 2001;2:746–56.

[92] Lesniewska E, Milhiet PE, Giocondi MC, Le Grimellec C. Atomic force microscope imaging of cells and membranes. Atomic Force Microscopy in Cell Biology 2002;68:51–65.

[93] Domke J, Dannohl S, Parak WJ, Muller O, Aicher WK, Radmacher M. Substrate dependent differencs in morphology and elasticity of living osteoblasts investigated by atomic force microscopy. Colloid Surfaces B 2000;19:367–73.

[94] Hinterdorfer P. Molecular recognition studies using the atomic force microscope. Atomic Force Microscopy in Cell Biology 2002;68:115–39.

[95] Ng L, Grodzinsky A, Plaas A, Sandy J, Ortiz C. J Struct Bio (in press).

[96] Seog J, Dean D, Plaas A, Wong-Palms S, Grodzinsky A, Ortiz C. Macromolecules 2002;35:5601-5615.

[97] Sneddon IN. The relation between load and penetration in the axisymmetric boussinesq problem for a punch of arbitrary profile. International Journal of Engineering Science 1965;3:47–57.

[98] Willemsen OH, Snel MM, Cambi A, Greve J, De Grooth BG, Figdor CG. Biomolecular interactions measured by atomic force microscopy. Biophys J 2000;79:3267–81.

[99] Marshall BT, Long M, Piper JW, Yago T, McEver RP, Zhu C. Direct observation of catch bonds. Nature 2003.

[100] Evans E. Probing the relation between force, lifetime and chemistry in single molecular bonds. Annual Review of Biophysics and Biomolecular Structure 2001;30:105–28.

[101] Merkel R, Nassoy P, Leung A, Ritchie K, Evans E. Energy landscapes of receptor-ligand bonds explored with dynamic force spectroscopy. Nature 1999;397:50–3.

[102] G. Bao, S. Suresh, 2003, Cell and molecular mechanics of biological materials. MIT Nature Materials, 2003;2:715–25.

[103] Glenister FK, Coppel RL, Cowman AF, Mohandas N, Cooke BM. Blood 2002;99:1060-1063.

[104] Cooke BM, Mohandas N, Coppel RL. Adv Parasitology 2001;50:1-86.

[105] Freyman TM, Yannas IV, Yokoo R, Gibson LJ. Fibroblast contraction of a collagen-GAG matrix. Biomaterials 2001;22:2883–91.

[106] Guck J. Private communication with K.J. Van Vliet, 2003.